International Journal of Engineering Science Invention (IJESI)
ISSN (Online): 2319-6734, ISSN (Print): 2319-6726
www.ijesi.org ||Volume 10 Issue 11 Series II || November 2021 || PP 08-17

Studies on human body effects on a printed UWB microstrip antenna, and SAR analysis in WBAN applications.

N.Sheshaprasad[1] and S. B. Bhanu Prashanth[2], Senior Member IEEE
[1]*Department of Electronics and Communication, B. N. M. Institute of Technology, Bangalore, India:*
[2]*Department of Medical Electronics, B. M. S. College of Engineering, Bangalore, India.*

ABSTRACT:*The impacts of the human body on the radiation parameters of a microstrip patch antenna constructed on a Roger RT5880 substrate with a relative permittivity of 2.2, as well as SAR analysis, are described in this work. The antenna was designed using the CST Microwave Studio suite environment, and it was printed using MITS electronics' Eleven Lab antenna printing equipment. The ground-plane width of the antenna was optimized to resonate at four frequencies: 2.4 GHz, 6.04 GHz, 8.63 GHz, and 13.95 GHz. With such multi band response and a wide bandwidth, antenna also gives VSWR less than 2 and -10dB return loss (S_{11}). The printed antenna was placed near human body in both simulation and real, to assess its performance characteristics. The SARs at 2.4 GHz and 5.8 GHz for a 10mW input power are 0.6381W/Kg and 1.42899 W/Kg, respectively, which is lower than the IEEE standard value of 1.6W/Kg for 1gram of tissue mass. As a result, this antenna is recommended as a candidate for use in Wireless Body Area Networks (WBAN) that operate in the Ultra-wide band frequency range.*

KEYWORDS-*Multi band antenna, SAR analysis, UWB, Wireless Body Area Network and communication.*

Date of Submission: 04-11-2021 Date of Acceptance: 18-11-2021

I. INTRODUCTION

The exponentially growing applications of wireless communications have resulted in the need of novel, multi-functional and multi-band antennas. In this context, the microstrip antennas offer a competitive solution with several advantages like low form-factor and cost, ease of manufacture and integration into a compact system [1-5]. Such antennas can communicate with multiple devices operating at different frequencies [6-11], and this has opened new avenues of research on multiband and ultra-wideband (UWB) antennas [12-20]. These antennas are reported to cover diverse technologies like WiMAX (3.4-3.6, 3.7-4.2GHz), Wi-Fi (3.6-3.7GHz) and WLAN (5.3-6.3GHz).

The Wireless Body area networks (WBAN) employ many wearable sensors with integrated wireless communication features and are predicted to have a greater impact on personal healthcare in near future. The smart sensor nodes measure different physiological conditions and communicate data to the personal digital assistant worn by the subject, or to a nearby router for further continuous health monitoring and analysis. Since the antennas in these applications operate on and around the human body, their performance may get affected due to the dispersive nature of the human body tissue.

Many antenna designs have been proposed in literatures for WBAN applications. A CPW fed antenna [21] at 2.45GHz has been studied inside the body for path loss in the human body of heterogeneous model. With a return loss of 24.45 decibels and a gain of 2.06 decibels, the flexible patch antenna [22] with split-triangle shape has been created for Wi Max applications. For WBAN applications with low SAR for on-body applications, a foldable UWB antenna [23] was developed. For WBAN communication, a metamaterial-based antenna with 2 X 2 H-shape unit cell [24] has been developed that resonates at 3.2GHz to 3.5GHz and 3.9GHz to 4.3GHz. For on-body applications, a rectangular microstrip antenna with Swastika slit [25] and a microstrip antenna at ISM 2.4 GHz [26] have been developed.

II. MATERIALS AND METHODS

This article describes the design, testing, and results of a microstrip antenna that operates between 2 and 6.6 GHz and is built on a Roger RT5880 substrate with a thickness of 1.6mm. The performance of the antenna near the human body has been confirmed in both modelling and real-world scenarios. The antenna was printed using MITS Electronics' Eleven Lab antenna printing equipment utilizing the optimal design values.

III. ANTENNA DESIGN SPECIFICATIONS

The initial operating frequency was chosen as 8.6 GHz. The mechanical dimensions & related parameters of the patch were calculated [18] using the governing relations (1) through (6) listed in Table 1.

The resonant frequency is less influenced by the variation in the width of the antenna [18]. Hence to design a square patch, the dimensions of Length and Width are optimized as Lp=11mm and Wp=11mm. Many techniques are recommended for feeding the antenna to match the input impedance of the antenna with the feed point for achieving maximum power transfer and high efficiency. Quarter wave transition technique with Microstrip line feeding [18] is used in our design to match the antenna impedance with the 50ohm line impedance.

To match the 50-ohm impedance of the line, the optimized width of 2 mm and length of 10 mm are calculated for feeding the antenna. The quarter wave transition length and width are 5mm and 1mm respectively. The substrate dimensions and ground plane dimensions are designed to be Ws=Wg=20 mm, Ls==Lg=30 mm. The patch and ground plane view of the designed basic square patch antenna and its dimensions are shown in Figure 1.

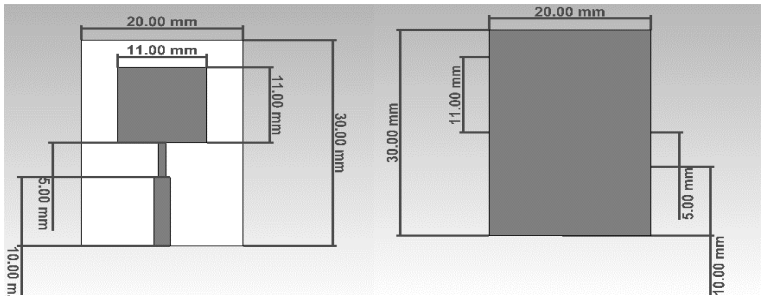

Figure 1. Front and rear view of the radiating antenna

IV. DEVELOPMENT OF PROPOSED ANTENNA

In the first step, a square patch antenna 1 (A1) with full ground plane is designed which resonates at 8.54GHz. As the intended antenna is for wide band purpose, the antenna A1 is modified by introducing notches and by reducing the ground plane with parametric analysis to obtain antenna A2. This antenna shows a bandwidth of 4.479GHz with S_{11} below -10dB. Further, slots and notches were introduced on patch as well as ground plane to obtain the proposed antenna A3 which resonates at multi bands, 2.4 GHz, 6.04GHz, 8.63GHz and 13.95GHz. The development stages from A1 to A3 are depicted in the Figure 2.

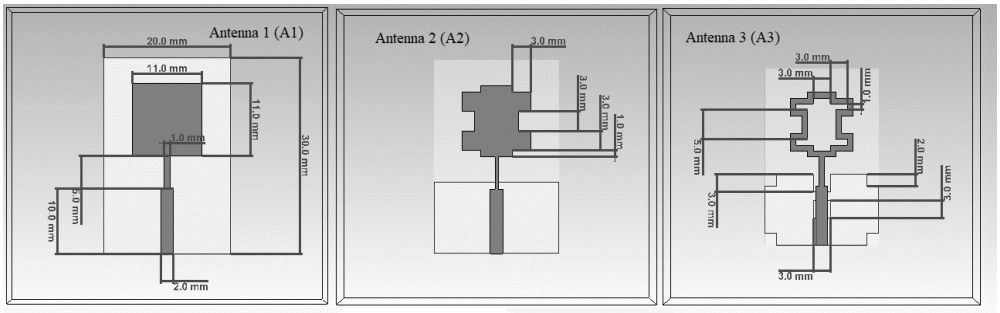

Figure 2. Front and rear view of the development of patch antennas A1, A2 and A3

TABLE 1. DIMENSIONS OF THE PRINTED ANTENNA

Eq. No	Design Parameter	Governing Equation	Value in mm
1	Width of the Patch	$W = \frac{c}{2fr\sqrt{\frac{2}{\varepsilon_r+1}}}$	13.78
2	The wavelength	$\lambda_0 = \frac{C}{f_r}$ C is the velocity of light and fr is the resonant frequency	34.88
3	Effective relative permittivity	$€reff = \frac{€r+1}{2} + \frac{€r-1}{2}\left[1+12\frac{h}{W}\right]^{-\frac{1}{2}}$ relative permittivity of substrate is 2.2 and height of substrate is 1.6mm	2.01
4	Length extension	$\Delta L = 0.412h\frac{(€reff+0.3)\left(\frac{W}{h}+0.264\right)}{(€reff-0.258)\left(\frac{W}{h}+0.8\right)}$	0.82
5	Effective length of antenna	$Leff = \frac{C}{2fr\sqrt{€reff}}$	12.30
6	Length of the patch	$L = Leff - \Delta L$	10.66

V. RESULTS AND DISCUSSION

The important parameters of antenna performance are gain, efficiency, VSWR, return loss (S_{11}) and directivity. Figure 3 illustrates the return loss S_{11} against frequency response of the basic patch antenna A1, with a single resonance frequency of 8.543 GHz and a relatively narrow bandwidth of 8.37 GHz – 8.69 GHz. This result is not promising for the planned Ultra Wide Band requirement.

Several approaches have been published in the literature to increase the antenna's bandwidth [19-20].In this work, the approach of using partial deformed ground plane, with slots and notches has been chosen to modify the basic patch antenna design. A parametric analysis was conducted to get the optimized effective ground plane to a width Wg=20 mm and length Lg=11 mm. The S_{11} graph for antenna A2 is shown in Figure 3.

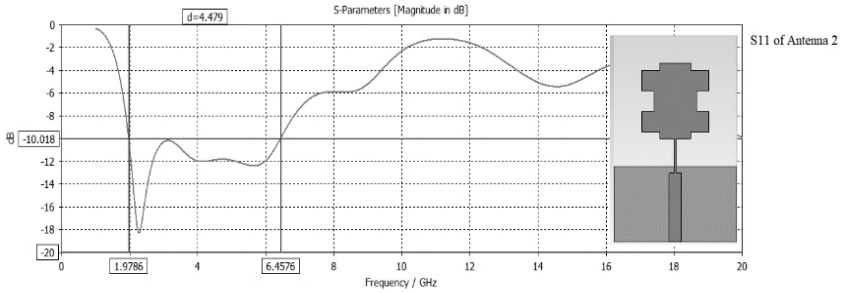

Figure 3. S_{11} Vs Frequency graph of Patch antenna A2

For the proposed antenna design A3, parametric analysis was conducted, and the dimensions of the center and corner slots were found to be 2.5 mm x 2.00 mm. The antenna resonates at four frequencies namely 2.4 GHz, 6.04GHz, 8.63GHz and 13.95GHz, and this is depicted in Figure.4 along with an inset of the slotted antenna device.

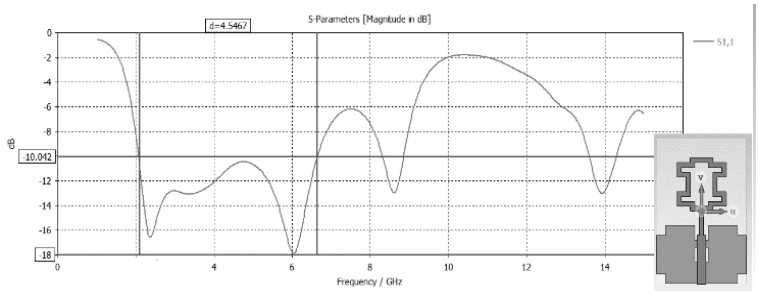

Figure 4. Graph of proposed antenna A3 with simulated return loss S_{11} vs frequency.

Table 2 lists the different characteristics simulated in free space, that is, without the effect of the human body, for these four resonant frequencies.

TABLE 2. FREE-SPACE SIMULATION RESULTS FOR THE A3 ANTENNA'S PARAMETERS

Antenna	Resonant Frequency (GHz)	Gain (IEEE) (dB)	Reflection Coefficient S_{11}(dB)	VSWR	Radiation Efficiency
Microstrip antenna A1	8.543	6.818	-24.39	1.18	-0.839dB 82.42%
Proposed antenna A3	2.4	0.522	-16.52	1.35	-2.687dB 53.86%
	6.04	0.8776	-17.84	1.29	-1.50dB 70.80%
	8.63	4.19	-12.95	1.58	-0.2575dB 94.24%
	13.95	3.484	-13.02	1.57	-0.7770dB 83.62%

The proposed antenna has multi band response and shows a wide bandwidth with VSWR of less than 2 and return loss S_{11} below -10dB as desirable for the UWB and WBAN applications. Hence the simulated antenna was fabricated for testing.

VI. DESIGN FABRICATION, TESTING AND RESULTS

The designed antenna shape was exported from CST to the MITS Design Pro software in gerber / dxf data. The antenna was subsequently milled by eliminating excess copper on a two-sided (Copper) Roger 5880 utilizing MITS electronics' Eleven Lab antenna printing machine in the, RF Microwave & Antenna design Prototype and Test Lab, founded in the department of ECE, BNMIT, supported by AICTE-MODROBS. After printing the antenna, an SMA connector was connected to the feed of the designed patch antenna. The setup used for printing of antenna is depicted in Figure 5, along with the measurement setup.

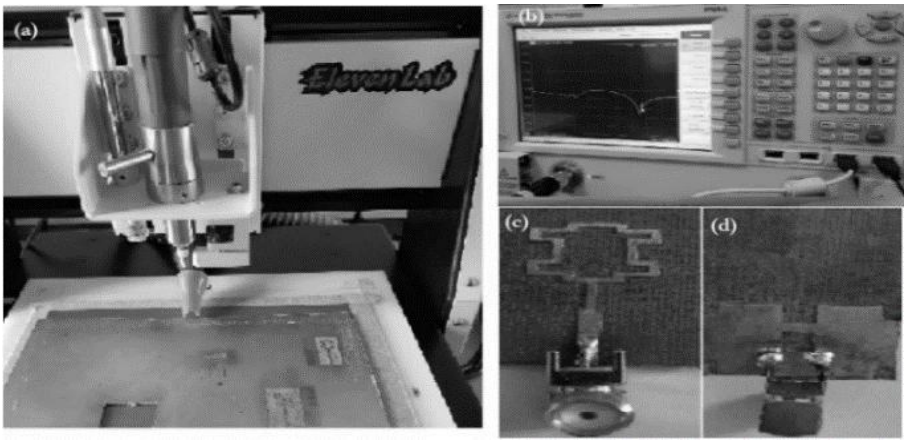

Figure 5. Fabrication and return loss measurement setup:(a) Antenna milling Machine (b) Network analyzer (c) and (d) Front and Rear views of the printed antenna

The printed antenna was then tested for return loss (S_{11}) measurement using Keysight's PNA-L N5232A Network analyzer in the Advanced RF and Wireless Communications research lab established in the department of ECE, BMSCE. It showed S_{11}'s of -18dB at 2.4GHz, -27dB at 5.8GHz and -11dB at 9GHz, and hence less than -10 dB in a wide bandwidth from 2GHz to 6.6GHz. There are small variations between simulation and measurement due to the feed network insertion loss and SMA connector insertion loss, which is shown in Figure 6.

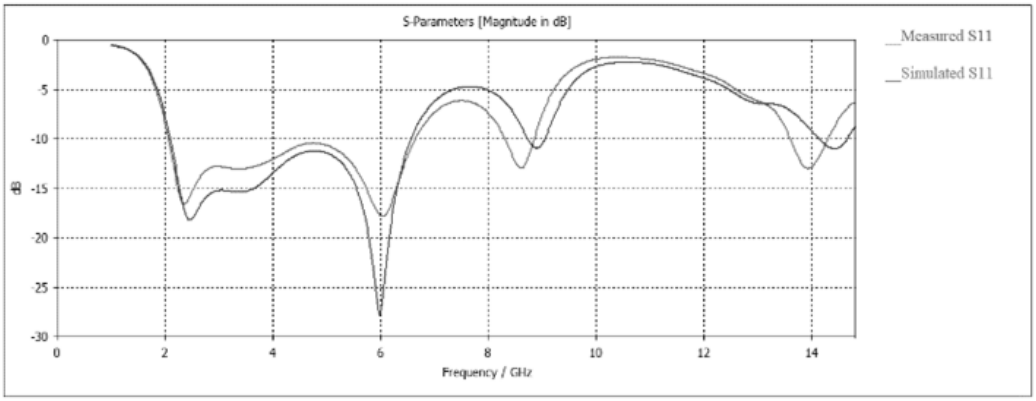

Figure 6. Return loss Vs Frequency graph of simulated and fabricated antenna

VII. SAR CALCULATIONS NEAR HUMAN BODY

This section is dedicated to investigations of the proposed slotted antenna performance by placing it in the vicinity of human body. The CST Voxel Family [32] has seven human model voxel data sets created for different stature, age and gender as in Figure 7. For simulation, 43-year pregnant female (Katja) voxel CST model was chosen to emulate a human body subject. The obtained results were compared with a multi-layer homogeneous model, serving as reference, having the 3-tissue layer layout [7]. The fabricated antenna was also placed on the real human hand and tested.

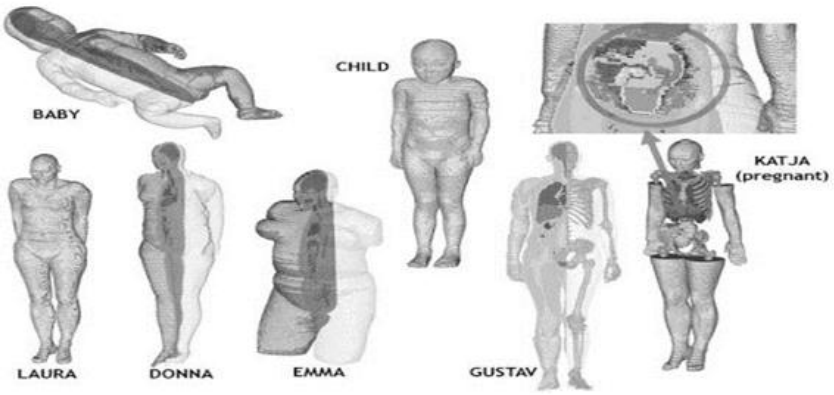

Figure 7. CST Voxel family

The industrial, scientific, and medical (ISM) band recommends 2.4GHz and it is widely used for many applications in the area of wireless body area networks, while the 5G wireless communication technology uses 5.8GHz. The antennas designed in these frequency bands are also used with the wearable devices for monitoring the human health conditions. The energy absorption rate by tissue is calculated using the index Specific Absorption Rate (SAR)[10], which is defined as the power absorbed per unit of tissue volume, as shown in equation 7.

$$SAR = \frac{P}{\rho} = \frac{\sigma|E^2|}{\rho} \qquad (7)$$

where P is the absorbed power in the tissue [W], E is the magnitude of the electric field strength vector [V/m], ρ is mass density of the medium [kgm-3], σ is electrical conductivity [S/m].

The measurement of SAR and calculation of other antenna parameters were performed at 2.4GHz and 5.8GHz for four cases of human body-antenna distances, as detailed next.

Case (1): The antenna was placed at 2mm from the 3 layer homogeneous body tissue model, consisting of Muscle, Fat and skin. The dielectric properties and the dimensions of these tissue layers are given in Table 3.

TABLE 3. TISSUE PROPERTIES [7]

Tissue	Conductivity (S/m)		Permittivity		Tissue dimension
	At 2.4GHz	At 5.8GHz	At 2.4GHz	At 5.8GHz	
Skin	1.44	3.72	38.10	35.1	50x50x2mm
Fat	0.268	0.837	10.8	9.85	50x50x4mm
Muscle	1.71	5.08	52.8	48.5	50x50x17mm

The antenna fully detunes, as illustrated in Figure 8, since the human tissue impacts the antenna's properties because it is comprised of different dielectric constants.

The SAR of 31.9092 W/Kg is measured when the antenna was at 2mm distance from a 3 layer tissue model of volume 57500 mm3 (50mmx50mmx23mm) with an input power of 0.5W at 2.4GHz as and the SAR at 5.8GHz is 71.4497 W/Kg, which is more than the IEEE guideline of 1.6 W/Kg for 1gram mass and is extremely dangerous to humans. Hence we have reduced the input power of the antenna and in each case, the SAR value is noted and tabulated in Table 4.

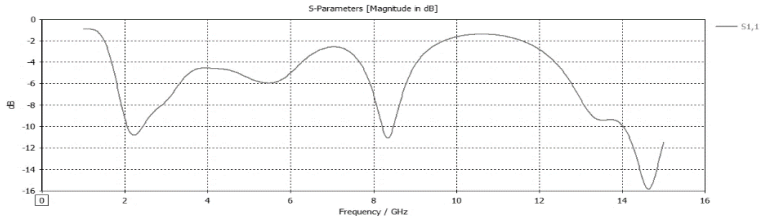

Figure 8. Return loss Vs Frequency graph of proposed antenna at 2mm from Body Tissue

TABLE 4. SAR VALUES AT DIFFERENT INPUT POWERS

Input Power in Watts	SAR @ 2.4GHz in W/Kg	SAR @5.8GHz in W/Kg
0.5	31.9092	71.4497
0.1	6.38185	14.2899
0.05	3.19092	7.14497
0.025	1.59546	3.57248
0.010	0.638185	1.42899

When the antenna was 2mm away from a 3-layer tissue model of volume 57500 mm^3 (50mmx50mmx23mm) with an input power of 10mW at 2.4GHz, the SAR was 0.638185 W/Kg, and the SAR at 5.8GHz was 1.42899 W/Kg, which is less than the IEEE accepted value of 1.6W/Kg for 1gram mass.

Case (2): The antenna was gradually pushed away from the bodily tissue until it was 40mm distant. The antenna parameters improve at this distance and the return loss graph of simulation is similar to free space return loss. A further increase in the distance has no effect on the bandwidth and it remains same as it was measured in free space. Hence the distance is fixed at 40mm.The SAR measured at 2.4 GHz and 5.8 GHz are 1.22066W/Kg and 0.896802W/Kg for 1gram mass at 40mm distance from body tissue with an input power of 0.5W as shown in Figure 9.

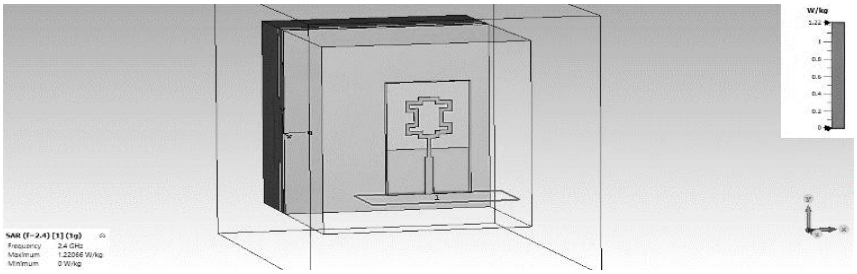

F**igure 9**. SAR @2.4GHz measurement at 40mm from body tissue

Case (3): The designed antenna was placed 2mm and 40mm away from Katja's hand for 2.4GHz and 5.8GHz frequency. All the parameters of the antenna and SAR was measured. For both the cases the results simulated are tabulated in Table 5. SAR value also depends on the antenna-human body distance, and the dielectric constants of the tissue layers. With an input power of 0.5W, the SAR value is higher when the antenna is close to the human body (17.0702W/kg and 45.9548W/kg at 2.4GHz and 5.8GHz, respectively, for 1gram mass at 2mm) and lower when the antenna is far from the human body (1.0731W/kg and 0.626275W/kg at 2.4GHz and 5.8GHz, respectively, for 1gram mass at 40mm). The SAR recorded at 2.4GHz at a distance of 40mm from the human body is shown in Figure 10.

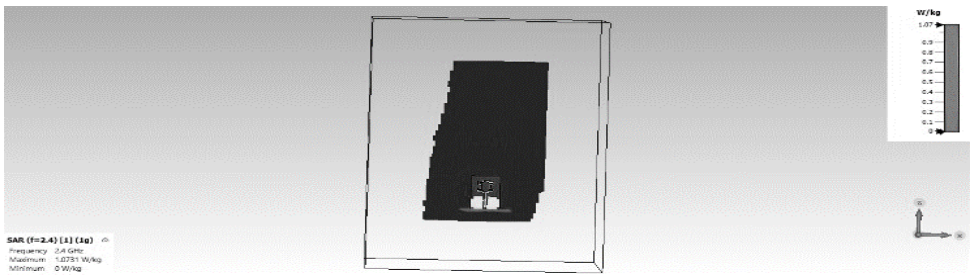

Figure 10. SAR measured when antenna placed at 40mm distance from Katja's hand at 2.4GHz.

Case (4): The printed antenna was placed on the real hand at 2mm and 40 mm and return loss was measured using Keysight's PNA-L N5232A Network analyzer. The fabricated antenna has return loss S_{11} of -24.9dB at 2.4GHz and -11.6 dB at 5.8GHz.

Due to significant power absorption by biological tissues, the antenna's efficiency is quite low when held very close to the human hand (19% at 2.4GHz and 39% at 5.8GHz). As the distance between the hand and the antenna grows, the radiation efficiency and gain are measured to rise. The average radiation efficiency is 42% and gain is 62% at 40mm distance.

In this experiment, the proposed antenna is safe to use on a human body at a distance of 40mm, and the average SAR value is considerably below the IEEE-specified RF safety exposure limit of 1.6W/kg. From 2.2GHz to 9.4GHz, the constructed antenna's S_{11} was less than -10dB, indicating a 7.2GHz band width. This is likely to be beneficial in a variety of WBAN applications, including the detection of brain tumors and breast tumors [30-31].

The insertion loss of the feed network and the SMA connection, as well as the impact of high dielectric values of real human body tissues compared to the simulation model, account for the discrepancy between measured and simulated findings.

The suggested antenna is small and has a large band width ranging from 2GHz to 6.6GHz, making it ideal for UWB on-body WBAN applications. Table 6 shows a comparison between past work and the proposed antenna.

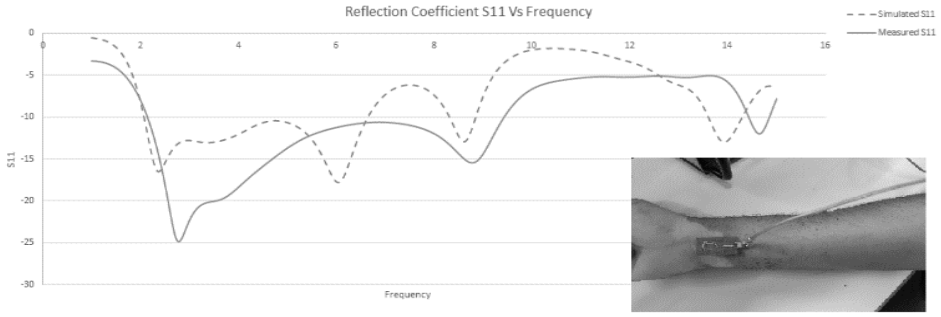

Figure 11. Return loss Vs Frequency graph of proposed antenna at 40mm from Hand

TABLE 5. ANTENNA PARAMETERS MEASURES AT 2mm AND 40mm DISTANCE FROM HAND OF KATJA

Antenna Parameters	2mm distance from hand of Katja		40mm distance from hand of Katja	
Frequency	at 2.4GHz	at 5.8GHz	at 2.4GHz	at 5.8GHz
Directivity (dBi)	2.804	8.800	3.526	6.285
Gain (IEEE) (dB)	-4.221	4.476	0.2177	4.683
Realized Gain (dB)	-4.672	3.592	-0.3146	4.182
Peak Surface Current (A/m)	50.09	47.87	47.013	37.81
Reflection coefficient $\|S_{11}\|$(dB)	12.12	11.09	13.30	17.38
VSWR	1.65	1.77	1.55	1.31
Radiation Efficiency (dB)	-7.025 19%	-4.054 39%	-3.308 46%	-1.602 69%
Total Efficiency (dB) and %	-7.476 17%	-5.208 30%	-3.804 41%	-2.103 60%
SAR(W/Kg) for 1g mass	17.0702	45.9548	1.0731	0.626275
SAR(W/Kg) for 10g mass	8.76184	11.6972	0.78214	0.435142

TABLE 6. COMPARISON OF PREVIOUS WORKS WITH PROPOSED ANTENNA DESIGN [24-29]**.**

Paper Reference. No.	Antenna Dimension in mm^3	Substrate	Frequency Range	Application
[24]	10 × 10 × 1.27	Rogers 3010	2.4 to 2.48 GHz	ISM Frequency Band
[25]	35 × 25 × 1.6	FR-4	UWB	UWB and On-Body WBAN
[26]	28 × 24× 1.6	FR-4	2.2–2.5 GHz	ISM Frequency Band
[27]	62 × 42 × 1.6	RT-Duroid 5880	3.2 to 3.5 GHz 3.9 to 4.3 GHz	WBAN and On Body
[28]	27 × 27 × 1	FR-4	4.2 to 12.5 GHz	UWB and WBAN On-Body
[29]	43 × 62 × 1.67	FR-4	2.3–2.4 GHz	WBAN
Proposed antenna	30 × 20 × 1.6	Rogers RT5880	UWB 2.2GHz to 9.4GHz	UWB and On-Body WBAN

VIII. CONCLUSIONS

CST MWS was used to simulate the results of a wide band microstrip antenna, and MITS antenna milling machine was used to build the antenna. The suggested manufactured antenna has an Ultra-Wide Bandwidth of 2GHz to 6.6GHz, as well as proper VSWR and return losses for wireless technologies. The suggested antenna has a compact size of 30 mm x 20 mm x 1.6 mm, and the observed SAR value complies with IEEE standards, making it ideal for WBAN applications.

ACKNOWLEDGMENTS

This work was supported by the Modernization of Advanced Communication Lab – RF, Microwave & Antenna Design, prototype and Test Lab, BNMIT, under AICTE Grant no.9-138/RIFD/MOD/policy –I/ 2018-19 dated 03.12.2019. The authors are thankful to the officials at Visvesvaraya Technological University in Belagavi, India, for their encouragement and help in completing this study.

REFERENCES

[1]. A. Pellegrini; A. Brizzi; L. Zhang; K. Ali; Y. Hao; X. Wu; C. C.Constantinou; Y. Nechayev; P. S. Hall; N. Chahat; M. Zhadobov; R.Sauleau, "Antennas and Propagation for Body-Centric Wireless Communications at Millimeter-Wave Frequencies: A Review",IEEE Antennas and Propagation Magazine, Vol. 55, I. 4, pp. 262 –287, 2013.

[2]. H. Liu ; J. Sarrazin ; F. Deshours ; T. Mavridis ; L. Petrillo ; Z.Liu ; P. D. Doncker ; and A. B-. Delaï, "Performance Assessment of IR-UWB Body Area Network (BAN) based on IEEE 802.15.6 Standard", IEEE Antennas and Wireless Propagation Letters, Vol. 15, pp. 1645 – 1648, 2016.

[3]. IEEE Standard for Local and metropolitan area networks _Part 15.6:Wireless Body Area Networks, pp. IEEE Std 802.15.6-2012, pp. 1 –271, 2012.

[4]. K. M. S. Thotahewa; J-. M. Redoutè; M. R. Yuce, "Propagation, Power Absorption, and Temperature Analysis of UWB Wireless Capsule Endoscopy Devices Operating in the Human Body", IEEE Transactions on Microwave Theory and Techniques, Vol. 63, I. 11, pp. 3823 – 3833, 2015.

[5]. P. A. Catherwood and W. G. Scanlon, "The Influence of the User in Body-Centric Antennas and Propagation at 3–6 GHz—A RicianKFactorApproach", IEEE Antennas and Wireless Propagation Letters, Vol. 13, pp. 907 – 910, 2014.

[6]. C. Kissi; M. Särestöniemi; C. P-. Raez; M. Sonkki; and M. N. Srifi,"Low-UWB directive antenna for Wireless Capsule Endoscopy localization", BodyNets2018 conference, Oulu, Finland, October 2018.

[7]. Hasgall PA, Di Gennaro F, Baumgartner C, Neufeld E, Lloyd B, Gosselin MC, Payne D, Klingenböck A, Kuster N, "IT'IS Database for thermal and electromagnetic parameters of biological tissues," Version 4.0, May 15, 2018, DOI: 10.13099/VIP21000-04-0.

[8]. T. Tuovinen ; M. Berg ; K. Y. Yazdandoost ; J. Iinatti, "Ultra wideband loop antenna on contact with human body tissues", IET Microwaves, Antennas & Propagation, Vol. 7, I. 7, pp. 588 – 596, 2013.

[9]. C95.1a-2010 - IEEE Standard for Safety Levels with Respect to Human Exposure to Radio Frequency Electromagnetic Fields, 3 kHz to 300 GHz Amendment 1: Specifies Ceiling Limits for Induced and Contact Current, Clarifies Distinctions between Localized Exposure and Spatial Peak Power Density, IEEE Std C95.1a-2010 (Amendment to IEEE Std C95.1-2005).

[10]. 95.2-2018 - IEEE Standard for Radio-Frequency Energy and Current-Flow Symbols, IEEE Std C95.2-2018 (Revision of IEEE Std C95.2-1999)

[11]. M. Särestöniemi; C. Kissi;C. P-. Raez ; T. Kumpuniemi ;M. Sonkki; S. Myllymäki ; M. Hämäläinen ; and J. Iinatti, "Measurement and simulation based study on the UWB channel characteristics on the hand area", accepted to be presented in ISMICT 2019 conference.

[12]. Y. Nijsure; W. P. Tay ; E. Gunawan ; F. Wen ; Z. Yang ; Y. L.Guan ; and A. P. Chua, "An Impulse Radio Ultrawideband System for Contactless Noninvasive Respiratory Monitoring", IEEE Transactions on Biomedical Engineering, Vol. 60, I. 6, pp. 1509 – 1517, 2013.

[13]. J. J. Liu; M-. C. Huang ; W. Xu ; X. Zhang ; L. Stevens ; N. Alshurafa ; and M. Sarrafzadeh, "BreathSens: A Continuous On-Bed Respiratory Monitoring System With Torso Localization Using an Unobtrusive Pressure Sensing Array", IEEE Journal of Biomedical and Health Informatics, Vol.19, I. 5, pp. 1682 – 1688, 2015.

[14]. Devesh Tiwari, Jamshed Aslam Ansari, Abhishek Kr. Saroj, Mukesh Kumar, "Analysis of a Miniaturized Hexagonal Sierpinski Gasket fractal microstrip antenna for modern wireless communications", AEU - International Journal of Electronics and Communications, Volume 123,2020, 153288, ISSN 1434-8411.

[15]. G. Varamini, A. Keshtkar, M. Naser-moghadasi, "Compact and miniaturized microstrip antenna based on fractal and metamaterial loads with reconfigurable qualification" AEUE – Int J Electron Commun, 83 (2018), pp. 213-221, 10.1016/j.aeue.2017.08.057.

[16]. Bidisha Hazarika, BananiBasu, and Arnab Nandi, "Design of Dual-Band Conformal AMC Integrated Antenna for SAR Reduction in WBAN," Progress In Electromagnetics Research C, Vol. 110, 91-102, 2021.

[17]. Kavneet Kaur, Ashwani Kumar, and Narinder Sharma, "Split Ring Slot Loaded Compact CPW-Fed Printed Monopole Antennas for Ultra-Wideband Applications with Band Notch Characteristics," Progress In Electromagnetics Research C, Vol. 110, 39-54, 2021.

[18]. C. A. Balanis,Antenna Theory: Analysis and Design, 4th ed., Hoboken,NJ, USA: Wiley, 2016.

[19]. Barbarino, S., Consoli, F. , 2012. UWB circular slot antenna provided with an inverted-L notch filter for the 5 GHz WLAN band. Prog. Electromagn.Res. 104, 1–13.

[20]. Chen, Y. , Yang, S., Nie, Z., 2010. Bandwidth enhancement method for low profile E-shaped microstrip patch antennas. IEEE Trans. AntennasPropag. 58 (July (7)).

[21]. Kurup, D., M. Scarpello, G. Vermeeren, W. Joseph, K. Dhaenens, F. Axisa, L. Martens, D. V. Ginste, H. Rogier, and J. Vanfleteren, "In-body patch loss models for implants in heterogeneous human tissues using implantable slot dipole conformal flexible antennas," EURASIP Journal on Wireless Commun. and Networking, Article number: 51 (2011), 2011.

[22]. Naik, K. K. and D. Gopi, "Flexible CPW-fed split-triangular shaped patch antenna for WIMAX application," Progress In Electromagnetics Research M, Vol. 70, 157–166, 2018.

[23]. Kang, C. H., S. J. Wu, and J. H. Tarng, "A novel folded UWB antenna for wireless body area network," IEEE Trans. on Antenna and Propag., Vol. 60, No. 2, 1139–1142, Feb. 2012.

[24]. Hazanka, B., B. Basu, and J. Kumar, "A multi-layered dual-band on-body conformal integrated antenna for WBAN communication," International Journal of Electronics and Communications, Vol. 95, 226–235, Oct. 2018.

[25]. Kumar, V. and B. Gupta, "On-body measurements of SS-UWB patch antenna for WBAN applications," International Journal of Electronics and Communications, Vol. 70, No. 5, 668–675, May 2016.

[26]. Ali, S. M., V. Jeoti, T. Saeidi, and W. P. Wen, "Design of compact microstrip patch antenna for WBAN applications at ISM 2.4 GHz," Indonesian Journal of Electrical Engineering and Computer Science, Vol. 15, No. 3, 1509–1516, Sept. 2019.

[27]. Liu, C., Y.-X. Guo, and S. Xiao, "Capacitively loaded circularly polarized implantable patch antenna for ISM band biomedical applications," IEEE Trans. on Antenna and Propag., Vol. 62, No. 5, 2407–2417, May 2104.

[28]. Terence, S., P. See, and Z. N. Chen, "Experimental characterization of UWB antennas for on-body communication," IEEE Trans. on Antenna and Propag., Vol. 57, No. 4, 866–874, Apr. 2009.

[29]. Abdulhasan, R. A., R. Alias, and K. N. Ramli, "A compact CPW fed UWB antenna with quad band notch characteristics for ISM band applications," Progress In Electromagnetics Research M, Vol. 62, 79–88, 2017.

[30]. Islam, M.T., Mahmud, M.Z., Islam, M.T. et al. A Low Cost and Portable Microwave Imaging System for Breast Tumor Detection Using UWB Directional Antenna array. Sci Rep 9, 15491 (2019). https://doi.org/10.1038/s41598-019-51620-z

[31]. S. A. Rezaeieh, A. Zamani, and A. M. Abbosh, "3-D Wideband Antenna for Head-Imaging System with Performance Verification in Brain Tumor Detection," IEEE Antennas and Wireless Propagation Letters, vol. 14, pp. 910–914, 2015.

[32]. http://www.mweda.com/cst/cst2013/mergedProjects/CST_EM_STUDIO/common_tools/bio_models.htm